Mustansiriyah Journal of Pure and Applied Sciences, Print ISSN: 2957-9910. Online ISSN: 2957-9929, Vol. 2, No. 3, 2024, Pages 116-135
DOI:

MJPAS

MUSTANSIRIYAH JOURNAL OF PURE AND APPLIED SCIENCES

Journal homepage:
https://mjpas.uomustansiriyah.edu.iq/index.php/mjpas

RESEARCH ARTICLE - physics

Study the Effect of Calcined Temperature on Structural, Optical and Magnetic Properties for Cobalt Ferrite Nanostructure

Ataa Jamal Mohammed [1]* , Suhad A. Hamdan[2]

[1,2] Department of Physics, College of Science, University of Baghdad, Baghdad, Iraq

* Corresponding author E-mail: Ataaalbakri@gmail.com

Article Info.

Article history:

Received
13 October 2023

Accepted
27 November 2023

Publishing
30 June 2024

Abstract

In this work, $CoFe_2O_4$ nanostructure was synthesized from Cobalt and ferric nitrates and sodium hydroxide (NaOH) by hydrothermal method. Effect of heat treatment on the structural, optical, and magnetic properties of the resulting powder was studied at calcination 400°C and 600°C with different concentration of NaOH. The resulted products were characterized by X-ray diffraction (XRD), Field emission scanning electron microscopy (FE-SEM), Fourier transformed infrared (FTIR), UV–Vis absorption, and vibrating sample magnetometer (VSM) technique as synthesis and when calcination at 400°C and 600°C with different concentration of NaOH. The absorption spectra show $CoFe_2O_4$ nanostructure absorb the ultra violet area. The high temperatures of the calcination process results in the reduction in crystallite size that their average crystallite size is found (11-14.26) nm. The FE-SEM images indicated that particles were agglomerated and spherical shape and size between (23.6 - 57.9) nm expect the morphology is clearly a structure nanorods at 3M at 400 °C. The created $CoFe_2O_4$ nanostructure have demonstrated ferromagnetic behavior for all the samples behavior which was found in VSM results examination.

The official journal published by the College of Education at Mustansiriya University

Keywords: Hydrothermal Synthesis, $CoFe_2O_4$ Nanoparticle, Magnetic Properties

1. Introduction

Cobalt ferrite (CoFe2O4) possesses a cubic spinel structure. In the inverse spinel configuration of the ferrite, Fe3+ ions usually live in the tetrahedral sites, while Co2+ and Fe3+ ions live in the octahedral sites (called B-sites) [1]. In order to manipulate the composition and microstructure of ferrite nanoparticles, it is imperative to employ several preparation methods [1]. CoFe2O4 nanoparticles have been synthesised using several methods in earlier studies, including sol-gel [2, 3], hydrothermal [4], chemical co-precipitation [5, 6], solvothermal [7], solid-state [8], and solution combustion [9–12] techniques

CoFe2O4 was studied because it has some interesting properties, such as high permeability, great electrochemical stability, amazing electrical and optical properties, and the ability to show different redox states [13,14]. These aforementioned features render it appropriate for a diverse array of applications [15, 16]. The properties of CoFe2O4 nanoparticles are determined by various factors, including the preparation method, morphology, particle size, heat treatment, and cation diffusion at tetrahedral and octahedral locations. These nanoparticles exhibit distinct and enhanced properties in electronic and electromagnetic device applications when compared to their bulk counterparts [17].

In this research, we have created a straightforward hydrothermal technique to produce cubic spinel $CoFe_2O_4$ nanoparticles. The impact of different calcined temperature and NaOH concentration on structural, optical, and magnetic properties of $CoFe_2O_4$

nanoparticles were investigated. The characteristics of the $CoFe_2O_4$ nanoparticles were studied to investigate their potential applications for use in advanced supercapacitors and photocatalytic oxidation of various dyes.

1. EXPERIMENTAL WORK

$CoFe_2O_4$ nanostructure was prepared from Cobalt and ferric nitrates using the hydrothermal method. The aqueous solutions of Cobalt nitrate hexahydrate with 0.2M was dissolved in distilled water and stirred in a magnetic stirrer until the solution appears pink. Ferric nitrate monohydrates (Iron nitrate nanohadrate) with 0.4M was dissolved in distilled water and stirred it until the solution appears orange. Dissolve NaOH with (1, 2, and 3) M in deionized water and stirred at 70^{o}C the resultant solution appears transparent. Then cobalt salt and iron salt were gradually added to NaOH boiled solution, then the pH of the solution was measured and its value was changed to 9. The resultant solution stirred for (6h) at 70 ^{o}C, the solution appears black. The resulting solution was placed in an autoclave and then placed in an oven at 100 ^{o}C for (3h). Resulting solution centrifuged for 30 min with 6000 revolutions per minute, then this process was repeated three times. Dried the resulting precipitate at 100 ^{o}C for 30 min, the material appeared in the form of a small black mass. The resulting substance was ground well and became a black powder, then annealed at 400^{o}C and 600^{o}C the resulting samples are ready for examined. These same steps were repeated different concentrations of NaOH. In the present study, $CoFe_2O_4$ nanostructure have been prepared by using the hydrothermal technique and annealed at various temperatures (400, and 600) ^{o}C. The purpose of this work is to examine how the annealing temperature affects morphological, structural, and optical properties of $CoFe_2O_4$ nanostructures synthesized. By using a Shimadzu version 4 (XRD) system, the structure related to the $CoFe_2O_4$ nanostructures was analyzed, and the intensity was recorded as a Bragg angle function. The radiation source was Cu (Kα) with λ= 1.5406 Å wavelength was used as the radiation source, while 40kV and 30mA were used for the voltage and current, respectively. The scanning angle 2θ was varied between 10 and 90 degrees step size 0.2 degree, at a speed of 10 degrees per min, with a preset time of 1.2 seconds. For analyzing the morphology regarding samples, a Field emission scanning microscope (FESEM) is used (MIRA3model-TE-SCAN (Dey Petronic Co.). The Fourier Transform Infrared (FTIR) test is employed to analyse the spectra of various substances. This is accomplished by utilising a Bruker FTIR analyzer, specifically the Tensor-27 model, manufactured by Bruker Optics Inc., located in Billerica, MA. The test is conducted in an attenuated total reflectance mode. The data were recorded in the range of wave number from 400 to 4000 cm^{-1}. To investigate the optical properties like absorbance-based absorbance spectra a UV-Visible spectrophotometer (190-1100) nm (Meterrech SP - 8001) was utilized. An AGFM-VSM model 117 was used for recording M-H curves regarding the samples during magnetic experiments with the use of a VSM.

2. RESULTS AND DISCUSSION

The cobalt ferrite nanostructure fabricated by employing a hydrothermal approach with 1 M of NaOH concentration and calcined for 0 ^{o}C, 400 ^{o}C and 600 ^{o}C are confirmed by the peaks observed in Fig. 1. The samples display the recognizable reflection from (220), (311), (222), (400), (422), (511), (440), and (533) planes, which are in good agreement with those of $CoFe_2O_4$ obtained from JCPDS card no. 96-591-0064.The peak (222) appeared at 0^{o}C , 400 ^{o}C and vanish at 600 ^{o}C. Another finding is that peaks shift to lower 2θ as the temperature of calcination rises, this shows that as thermal energy is added, the rate at which cobalt ions are incorporated into the lattice increases[18]. Due to the fact that the peak shift and

lattice constant vary depending on the substituted cations, this makes it possible to discriminate between the diffraction patterns of distinct spinel ferrites[19]. However, when the calcination temperature increased, the peak strength steadily dropped, indicating that the expansion of peaks was hampered by the rise in calcination temperature. The vibrating of the atoms in the sample may be directly connected to the drop in nanoparticle peak intensity as temperature rises[20]. Recently study[21] demonstrated how changing the distance between the nearest crystal planes (d) might result from an increase in atomic thermal vibration caused by an increase in temperature, and therefore the 2θ position of the diffraction peak also shifts from its original position; and the diffraction peak's intensity decreases. The high purity of the product is supported by the fact that the XRD spectra did not find any further impurity peaks[22]. The crystallite sizes have been calculated from the highest intensity (311) peaks utilizing

the Debye–Scherrer's formula [23][24] for all the cobalt ferrites calcined samples and the results were recorded in Table 1.

$$D = \frac{k\lambda}{\beta \cos\theta} \quad (1)$$

Where k = shape factor, λ = 1.54060Å, β = Full Width Half Maximum (FWHM) and θ = diffracting angle. The results showed that when the calcination temperature increased, the crystallite sizes had relatively reduced. The high temperatures of the calcination process may be to blame for the nanoparticles' cracking or fracturing, which results in the reduction in crystallite size[25]. By applying Bragg's Law to the X-ray diffraction (XRD) pattern, the lattice parameter was determined [26]. The symbol for interplanar spacing is "d," and the lattice parameter for the corresponding 2 peak position value is "a." The integers h, k, and l are commonly referred to as Miller indices [27].

$$a = d\sqrt{h^2 + k^2 + l^2} \quad (2)$$

Lattice constant has expanded from 8.39 to 8.53 Å. The substituted cations affect how the lattice constant behaves since the radius of Fe^{3+} (0.64 Å) is lesser thanCo^{2+} (0.72 Å) this answers the rising lattice constant with the introduce of cobalt cation into the lattice. [28]. According to a research [19], the lattice constant increased as the calcination temperature rose.

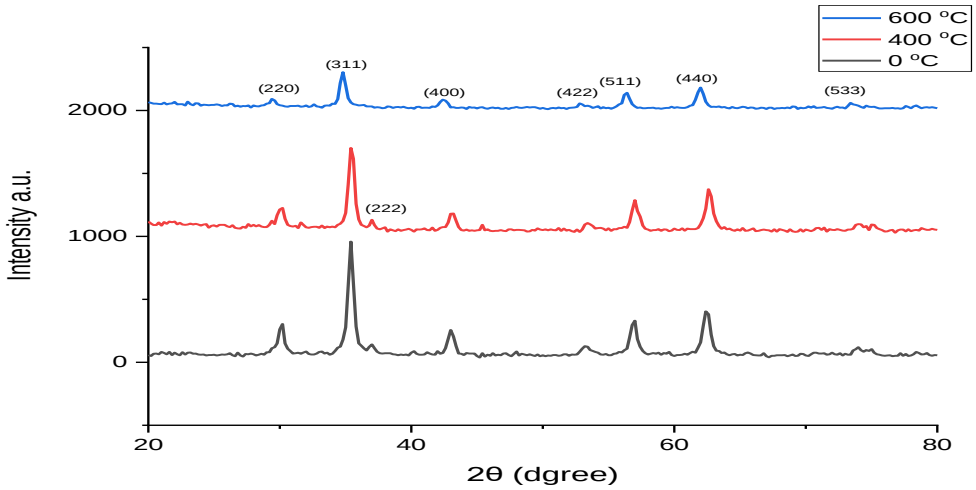

Figure 1: XRD of $CoFe_2O_4$ with different calcination temperature at 1 M NaOH

Figure 2 represents the XRD of the prepared cobalt ferrite nanostructure by hydrothermal with 3 M NaOH concentration and calcined at different temperature (0 ºC, 400 ºC, 600 ºC). The $CoFe_2O_4$ nanostructure appears structure with a comparison to the standard card (JCPDS card no. 96-591-0064). The samples demonstrate the typical reflection from (220), (311), (222), (400), (422), (511), (440), and (533) planes. Comparing the XRD patterns, It is noticed diffraction peaks are present of the calcinated sample at 600 ºC are narrower and more intense, this assumes that it enhances the crystallinity with the temperature of calcination is elevated[29][30]. An additional peak at 2θ 45.6° related to secondary impurities were observed for the sample calcined at 600 °C, which may have been driven on by sample degradation[31]. Cobalt ferrite was also calcined by an earlier study [19], and it had a peak at the same angle. Lima *et al* [30]also confirmed that the $CoFe_2O_4$ NPs presented a secondary phase during the synthesis. Since the creation of the impurity phase is inconsistent with the concentration of the substituent. As a result, it can be mainly linked to the synthesis or postsynthesis circumstances of the samples[32]. For all of the calcined samples, the crystallite sizes were determined from the highest intensity (311) peaks using equation (1), and the results are shown in Table (1). Table 1 showed that when the calcination temperature increased, the crystallite size relatively marginally reduced. This may be as a result of the presence of an impurity obtained by the oxidation process [33]. The super-exchange bonds between the magnetic cations break when an impurity or lack of oxygen ions are present at the surface, causing a significant surface spin disorder. The super-exchange interaction depends on the bond angles and bond lengths, this, clearly would differ near the surface due to the bonds' termination. As a result, the bond length and angle are broken when the super-exchange bonds are broken. A dead surface layer that reduces crystallite size and saturation magnetization may arise as a result of the disordered spin at the surface[34]. Equation (2) was used to get the lattice parameter from the XRD pattern. By raising the temperature of calcination, the lattice constant dropped, which may indicate that during cation migration during annealing, Fe^{3+} ions in tetrahedral sites migrate to octahedral sites and Co^{2+} ions in octahedral sites migrate to tetrahedral sites [35].

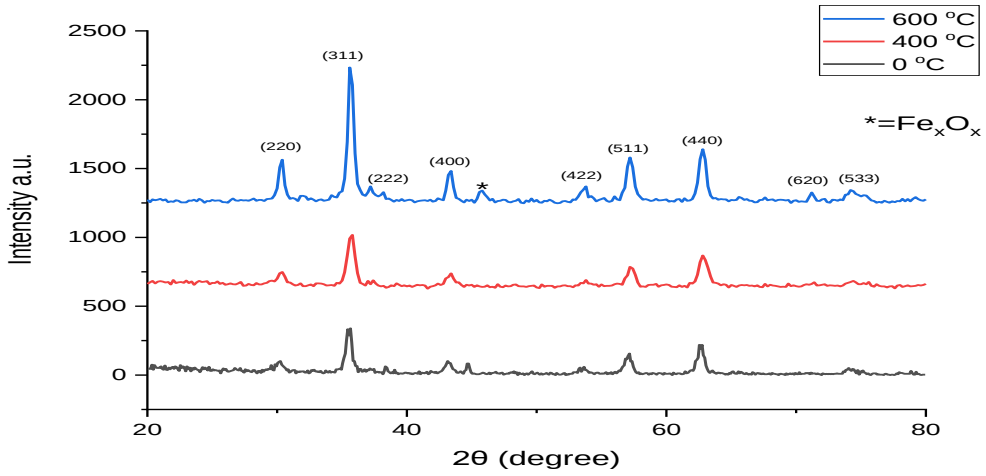

Figure 2: XRD of $CoFe_2O_4$ with different calcination temperature at 3 M NaOH

Figure 3 clearly demonstrates the XRD of the hydrothermally created cobalt ferrite nanostructure with 5 mol NaOH concentration and calcined at different temperature (0 ºC, 400 ºC, 600 ºC). The $CoFe_2O_4$

nanostructure appears structure with a comparison to the standard card (JCPDS card no. 96-591-0064). The diffraction spectra exhibit peaks of (220), (311), (222), (400), (331), (422), (511), (440), and (533) planes related to the cobalt ferrite cubic phase. From XRD patterns, it is evident that the calcination induces narrower and higher diffraction peaks, evidence of a rise in crystallinity [19][29][30]. Peaks at 2θ 20.6º, 29.4º, 34.1º, 39.6º and 45.6º represent to impurities that formation during synthesis or post-synthesis of the samples[32]. Because there were too many Fe ions after the synthesis process and not enough Co ions to occupy the octahedral sites in the spinel structure of the ferrite, α-Fe_2O_3 was present[36] According to a report [34], hematite is created when iron hydroxide reacts with air during calcination. The presence of α-Fe_2O_3 was previously reported in the literature [31][37][34]. In accordance with earlier articles[19][34]by raising the calcination temperature to 800 ºC or higher, the amount of cobalt ferrite impurities might be reduced and even eliminated. In order to determine the crystallite sizes for all of the calcined samples, the highest intensity (311) peaks were used, the findings are shown in Table (1). It was shown from table (1) that when calcination temperature increased, the crystallite size relatively reduced. Because of the presence of hematite might minimize crystallite size after calcination[38]. As mention above, The super-exchange bonds between the magnetic cations are broken when an impurity or an absence of oxygen ions are present at the surface, inducing a large surface spin disorder[39]. The disordered spin at the surface may result in the existence of a dead surface layer that decreases the crystallite size and saturation magnetization[33]. Equation (2) was used to determine the lattice parameter from the XRD pattern. The results indicated that the lattice parameter reduction with the increasing of calcination. Similar behavior of the lattice constant was observed by Prasetya *et al* [40].

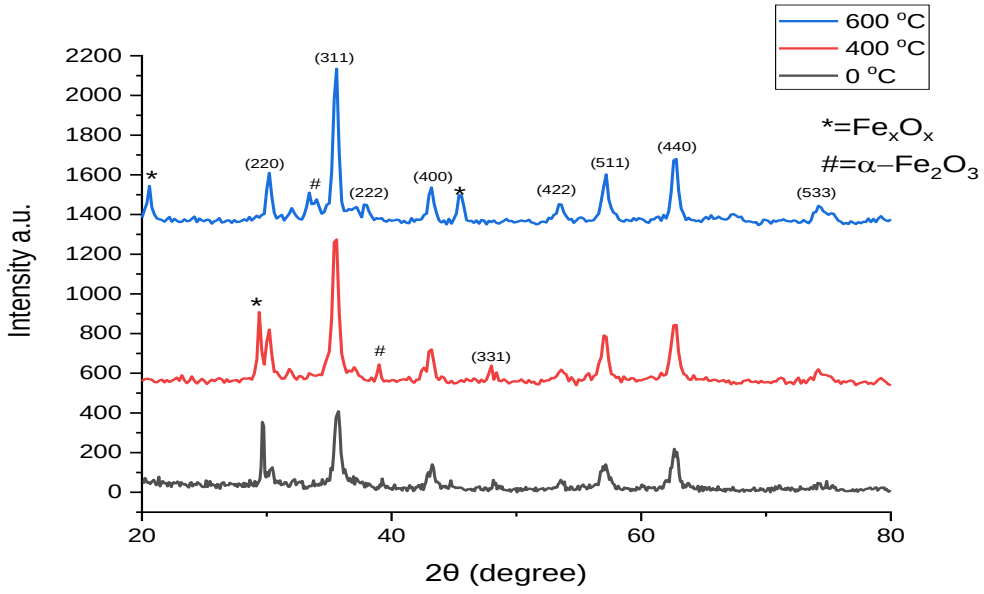

Figure 3: XRD of $CoFe_2O_4$ with different calcination temperature at 5 M NaOH

Table 1: Crystallite size and lattice constant of $CoFe_2O_4$ with different calcination temperature

Sample Name		2θ(degree)	FWHM β (degree)	D(nm)	Lattice Constant (a) Å
NaOH Concentration	**Calcined Temperature ºC**				
1 M	**0**	35.4226	0.6173	14.11	8.39
	400	35.468	0.6109	14.26	8.38
	600	34.8149	0.6218	13.98	8.53
3 M	**0**	35.54581	0.57108	15.26	8.59
	400	35.7153	0.749	11.64	8.55
	600	35.688	0.6394	13.63	8.33
5 M	**0**	35.66876	0.6167	14.13	8.42
	400	35.5208	0.6552	13.30	8.37
	600	35.5531	0.6205	14.04	8.36
JCPDS card		35.632			8.35

Figures (4, 5 and 6) shows calcinated cobalt ferrite nanostructures at (0, 400 and 600) ºC for (1, 3, 5 mol) of NaOH concentration presented in the range (4000-500) cm^{-1} have been investigated by FTIR spectroscopy at room temperature.

The well-known bands in the 3775-3426 cm^{-1}, 1616-1641 cm^{-1} and 1381-1385cm^{-1} range are assigned to the O–H stretching vibration indicating the existence of water adsorbed in the surface of the nanostructures [29], [32], [41]–[46]. The absorption bands at 2922-2935 cm^{-1} were observed, which are linked to the C–H stretches[19], [42]. Furthermore, the frequency band 583-587 cm^{-1} shows strong absorption and is assigned to vibration of the tetrahedral metal complex which comprised in a bond between the oxygen ion and the tetrahedral site metal ion[26], [35], [43], [47]. The fabrication of cobalt ferrite uses different molar concentrations of NaOH, as illustrated in Figures, which alters the absorption strength but stays in the same frequency range. This demonstrates that the different NaOH molar concentrations during the production of cobalt ferrite has the potential to modify its magnetic characteristics[48]. FTIR peaks of synthesized cobalt ferrite nanostructures were shown in Table (2).

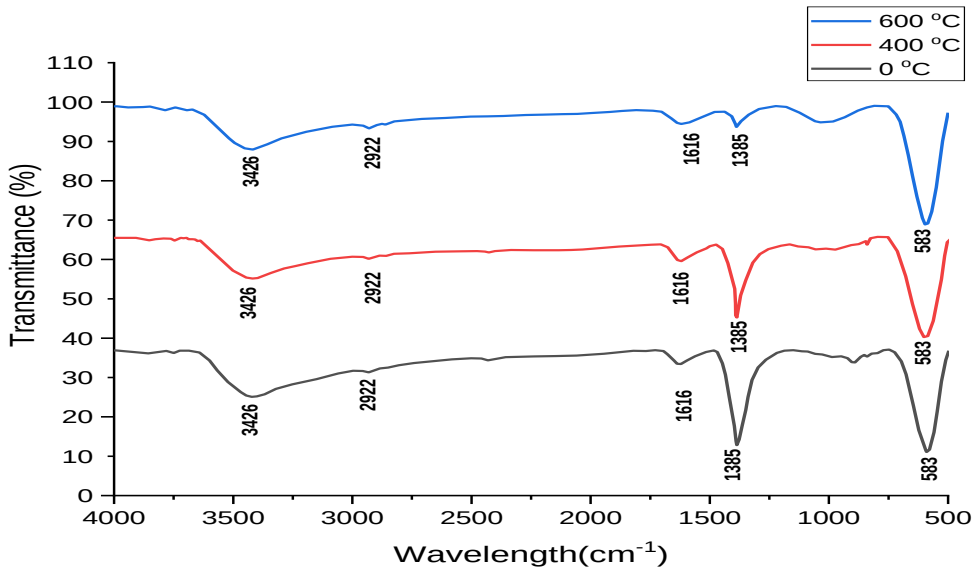

Figure 4: FTIR of $CoFe_2O_4$ with different calcination temperature at 1 M NaOH

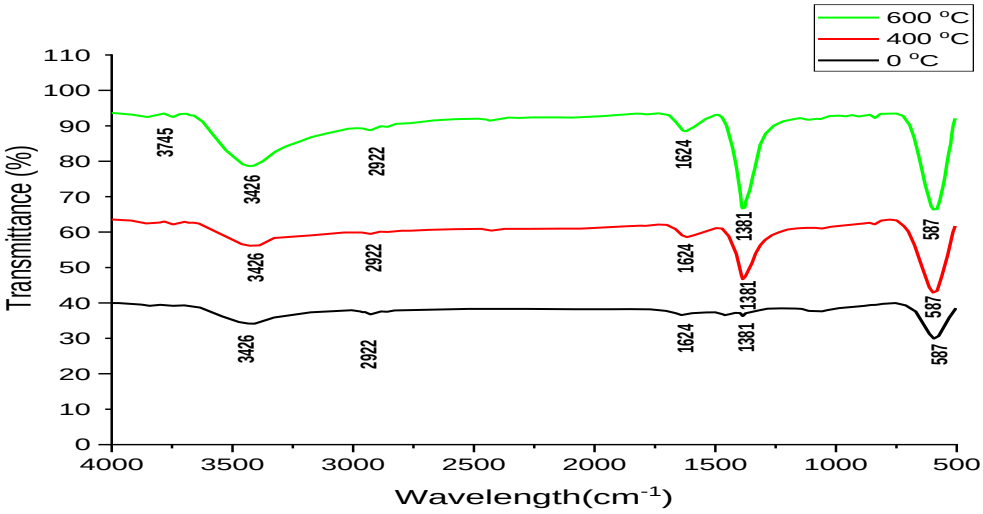

Figure 5: FTIR of $CoFe_2O_4$ with different calcination temperature at 3 M NaOH

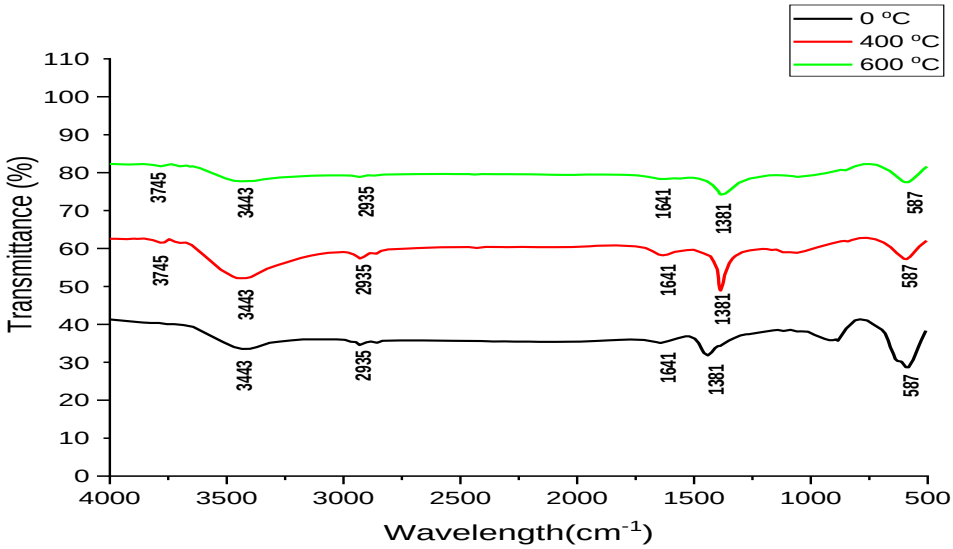

Figure 6: FTIR of $CoFe_2O_4$ with different calcination temperature at 5 M NaOH

Table 2: FTIR peaks of synthesized cobalt ferrite nanostructures

Chemical Bonds	**Band Location cm^{-1}**		
	1M	3 M	5 M
O–H stretching vibration		3745	3775
O–H stretching vibration	3426	3426	3443
C–H stretches	2922	2922	2935
O–H stretching vibration	1616	1624	1641
O–H stretching vibration	1385	1381	1381
Metal-Oxygen stretching vibrations	583	587	587

The optical absorbance of cobalt ferrite nanostructures synthesized with 1 mol of NaOH calcinated at 0, 400 and 600 °C temperatures is shown in Fig. (7) in the wavelength range of 200–800 nm. The absorbance is often influenced by a number of variables, including oxygen deficit, band gap, impurity centers, particle

size, lattice strain, and surface roughness[49]. However, the absorption spectra show that the products substantially absorb the ultra violet area, which is consistent with the findings of other studies [22]. The size and shape of various products of cobalt ferrite nanostructure may be the source of the tiny absorption discrepancies in the spectra of the samples[50].

The energy gap values were about 3.22, 2.96 and 2.65 eV for cobalt ferrite nanostructures with concentrations 1 mol NaOH calcined at (0, 400, and 600^{o}C), respectively. While, Rashmi *et al* [51]found the energy band is 4.1 eV. Furthermore, Saleem et al [52] were found energy band between 3.98 eV to 3.21 eV. Many other studies[53][54][55][56] were found energy band between 1.10-2.41 eV. The findings demonstrate that as calcination temperature is raised, $CoFe_2O_4$ nanostructure optical energy gap values decrease. This suggests that a drop in energy band gap value is connected with a rise in calcination temperature, possibly due to a quantum size impact. It is proposed that transitions between the valance and conduction bands may be the cause of the band gap reduction.[57]. While Habibi *et al*[58] explained a solid comprising Fe^{3+} and Co^{2+} ions might add a new level to the conduction band and the electrons could be promoted from the valence band to these ions levels, resulting in a narrowing of the band gap.

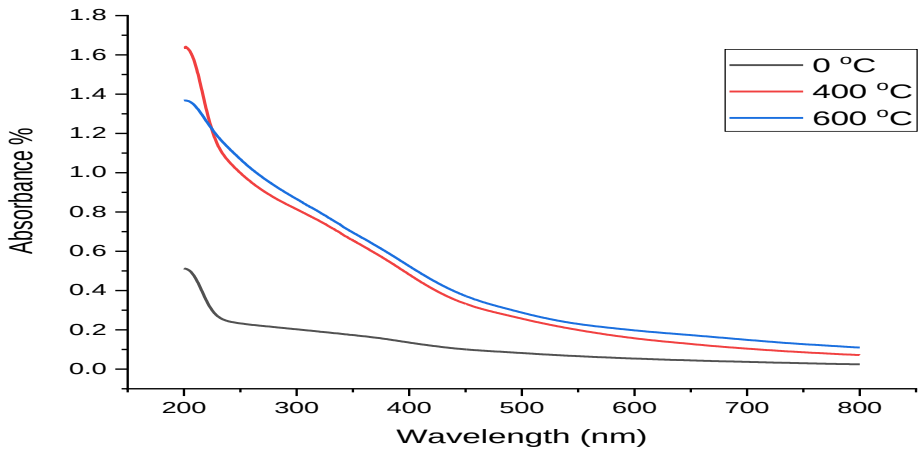

Figure 7: Absorption of $CoFe_2O_4$ with different calcination temperature at 1 Mol NaOH

The optical absorbance of cobalt ferrite nanostructures synthesized with 3 mol of NaOH calcinated at 0, 400 and 600 ^{o}C temperatures is shown in Fig. (9) in the wavelength range of 200–800 nm. The amount of oxygen, band gap, impurity centers, particle size, lattice strain, and surface roughness are several of the variables that affect absorbance in general.[49]. However, at the absorption spectra, it can be seen that the products highly absorb UV radiation, which is consistent with the findings of earlier studies[22]. The size and shape of various cobalt ferrite nanostructure products may be the origin of the modest absorption variations seen in the samples' spectra [50].

The energy gaps of cobalt ferrite nanostructure were determined from equation (3). The energy gap values were about 3.32, 3.37 and 3 eV for cobalt ferrite nanostructures with concentrations 3 mol NaOH calcined at (0, 400, and 600 ^{o}C), respectively (see Fig. (10)). Meanwhile, Rashmi *et al* [51]found the energy band is 4.1 eV. Saleem et al [52] were found energy band between 3.98 eV to 3.21 eV. Many other

studies[53][54][55][56] were found energy band between 1.10-2.41 eV. The results show that the optical energy gap values of $CoFe_2O_4$ nanostructure decrease relatively with increasing calcination temperature. Sugihartono *et al*[59] thought that the oxygen vacancy is responsible for the band gap's shrinking. Thus, the oxygen vacancy is caused by a disordered crystal structure at the high calcination temperature.

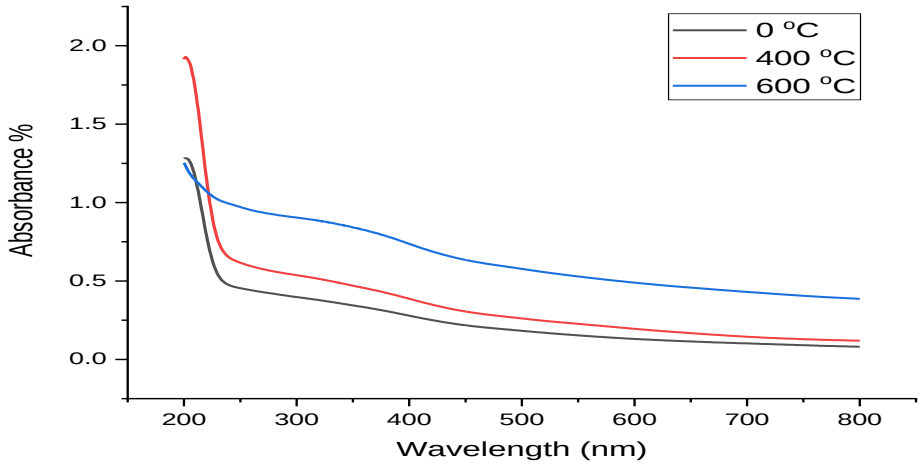

Figure 9: Absorption of $CoFe_2O_4$ with different calcination temperature at 3 Mol NaOH

The optical absorbance of cobalt ferrite nanostructures synthesized with 5 mol of NaOH calcinated at 400 and 600 ^oC temperatures is shown in Fig. (11) in the wavelength range of 200–800 nm. The absorbance is often influenced by a number of elements which is oxygen deficiency, band gap, impurity centers, grain size, lattice strain and surface roughness[49]. On the other hand, we can see from the absorption spectra that the products substantially absorb UV radiation, which is similar to previous study results [22]. The small absorption differences in the spectra of samples may be because of the size and morphology of different products of cobalt ferrite nanostructure [50].

The energy gaps of cobalt ferrite nanostructure were determined from equation (3). The energy gap values were about 3.44, 3.5 and 3.79 eV for cobalt ferrite nanostructures with concentrations 5 mol NaOH calcined at (0, 400, and 600^oC), respectively (see Fig. (12)). While, Rashmi *et al* [51]found the energy band is 4.1 eV. Saleem et al [52] were found energy band between 3.98 eV to 3.21 eV. Many other studies[53][54][55][56] were found energy band between 1.10-2.41 eV. The findings demonstrate that as the calcination temperature is raised, the optical energy gap values of the $CoFe_2O_4$ nanostructure decrease. These results are in agreement with earlier study[31]. The accumulation of NPs may be the cause of the band gap energy increase with temperature. The NPs' band gap energy rises as they are aggregated since this lowers their surface-to-volume ratio and, consequently, their capacity to absorb light. The creation of new structures inside the nanoparticles as a result of the calcination process is another possibility that might contribute to the impact that was seen [60]. Table (3) showed the value of energy gap of all samples.

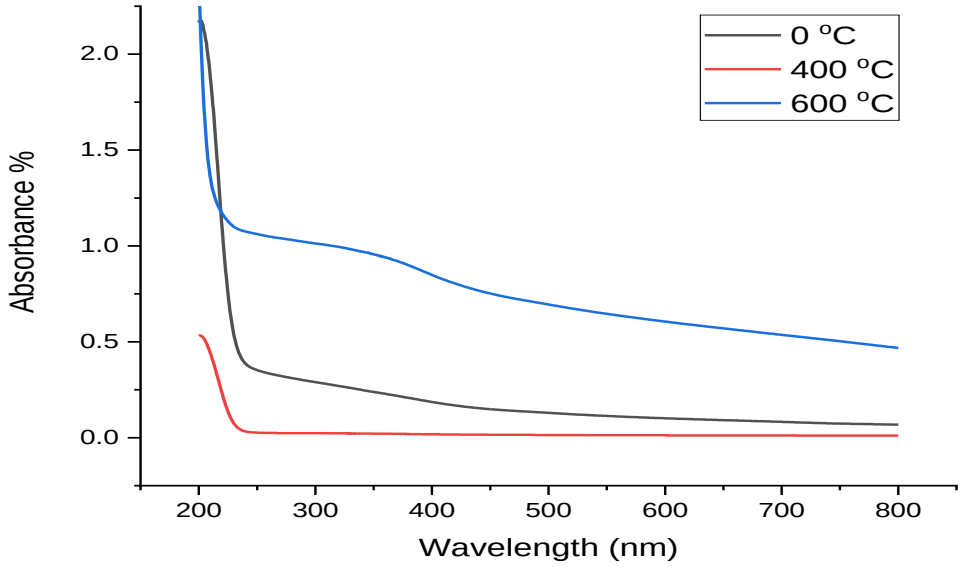

Figure 11: Absorption of $CoFe_2O_4$ with different calcination temperature at 5 Mol NaOH

Table 3: Value of energy gap of all samples

Sample Name		Optical Energy band (eV)
NaOH Concentration	**Calcined Temperature ºC**	
	0	3.22
1 Mol	**400**	2.96
	600	2.65
	0	3.32
3 Mol	**400**	3.37
	600	3
	0	3.44
5 Mol	**400**	3.5
	600	3.79

Figure (10) shows the FE-SEM micrographs of cobalt ferrite nanostructure synthesized with 1 M of NaOH calcinated at different temperatures. The FE-SEM images indicated that particles were agglomerated and spherical shape and size between 23.6 to 57.9 nm. The crystallite size determined from the X-ray diffraction data was less than the particle size that was seen. Because of the resultant agglomeration, which caused many crystallites to combine to create a bigger particle, as well as grain development at a higher calcination temperature, the Gibbs free energy coming from the reduction of extended surface area of nanoparticles is minimized [26]. Similar results were observed in previous studies [61][62][53][58].

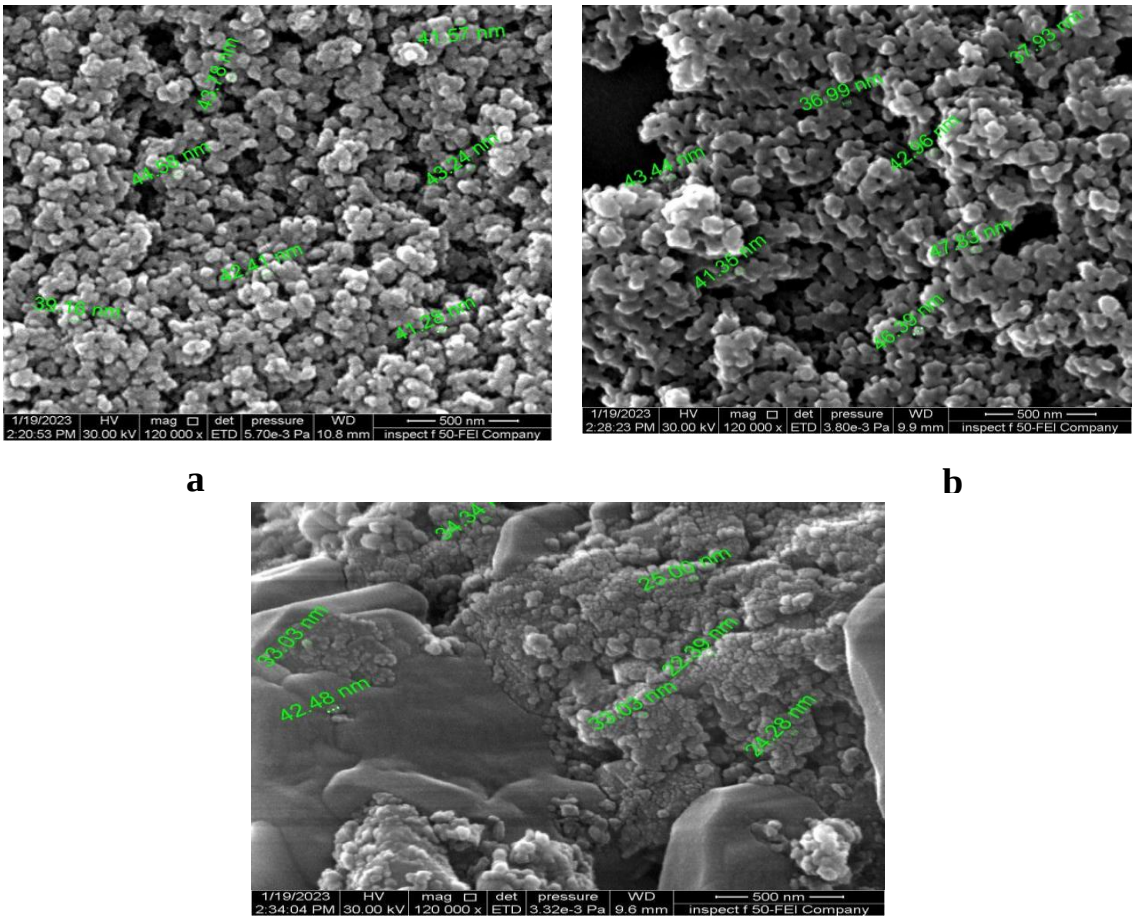

a **b**

c

Figure (10): FE-SEM images of $CoFe_2O_4$ with 1M concentration of NaOH (a) as synthesis (b) 400ºC (c) 600ºC

Figures (11) shows the FE-SEM micrographs of cobalt ferrite nanostructure synthesized with 3M of NaOH calcinated at 400 and 600 oC temperatures. It is clear in figure (11a) that nano-rods and spherical shapes are formed and agglomerated. The morphology is clearly a structure nanorods with a diameter of 78 nm and length of 533 nm which is similar to Pervaiz et al [63] results. The particle aggregations increased when the calcination temperature was raised to 600 ºC. Hence, that higher temperature inevitably causes moderate agglomeration [31].

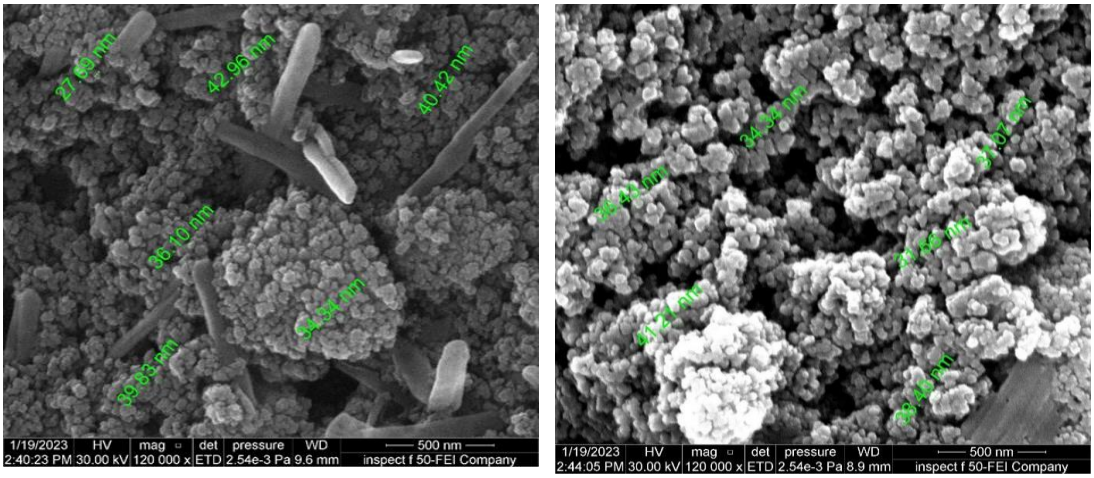

a **b**

Figure (11): SEM picture of $CoFe_2O_4$ with 3M concentration of NaOH calcined at (a) 400 ºC (b) 600 ºC

Figure (12) shows the FE-SEM micrographs of cobalt ferrite nanostructure synthesized with 5 mol of NaOH calcinated at 400 and 600 ºC temperatures. It is clear from Figure (12) that $CoFe_2O_4$ have uniform morphology with the individual particles have a particles size from 23 to 49 nm but there is agglomeration of particles. The magnetic contact and van der Waals interactions between the nanoparticles cause this aggregation[44][64]. Moosavi et al[34] explained magneto-dipole interactions between crystals and the presence of the hematite impurity caused the trend toward agglomeration to be seen.

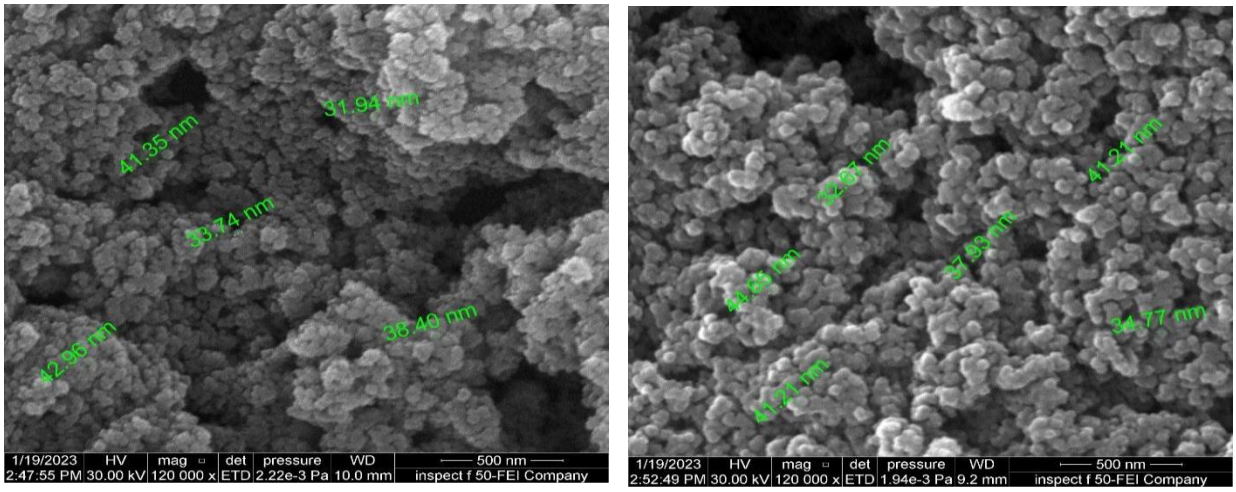

a **b**

Figure (12) SEM picture of $CoFe_2O_4$ with 5M concentration of NaOH calcined at (a) 400 ºC (b) 600 ºC.

Magnetic characterization of the cobalt ferrite synthesized with 1 M NaOH samples before and after calcination was performed using a vibrating sample magnetometer as showed in Figure (13). The cobalt

ferrite nanostructure's ferromagnetic characteristics before and after calcination were shown by the magnetic hysteresis that was discovered at room temperature. The coercivity H_C of the $CoFe_2O_4$ nanostructure samples without calcination was 439 Oe, and after calcination for 400 and 600 ºC, it increased to1740 and 1439 Oe respectively. The saturation magnetization (Ms) before calcination was 58 emu/g and after calcination it was 60 and 68 emu/g for 400 and 600 ºC respectively. the saturation magnetization values (Ms) are lower than the bulk $CoFe_2O_4$ (~80 emu/g)[34][65]. The interplay between the magnetic spin moment's surface order and disorder and the disruption to the spinel structural inversion brought on by Laplace pressure may be responsible for this decrease in saturation magnetization [66]. Table (3) showed the saturation magnetization and remenant magnetization increased with increasing calcination temperature. This resulted from the treatment at low temperatures' partial crystallization and tiny particle size. Hence, the particle size was increased with increasing calcination temperature which has been confirmed from FE-SEM analysis. Other elements, such as the high percentage of surface atoms, the unsaturated ligand, and the potent thermal disturbance properties, could also be play a role. Hence, it may be inferred that the magnetic configuration of the crystal exhibited instability and disorder, resulting in the inability to maintain a consistent magnetic moment in alignment with the external field [61]. The saturation magnetization can also rise with particle size because the powder surface contained a non-magnetic layer, and the proportion of the layer dropped as the particle size increased [61]. Reduced grain growth is the cause of the rise in coercivity with increased calcining temperature [67].

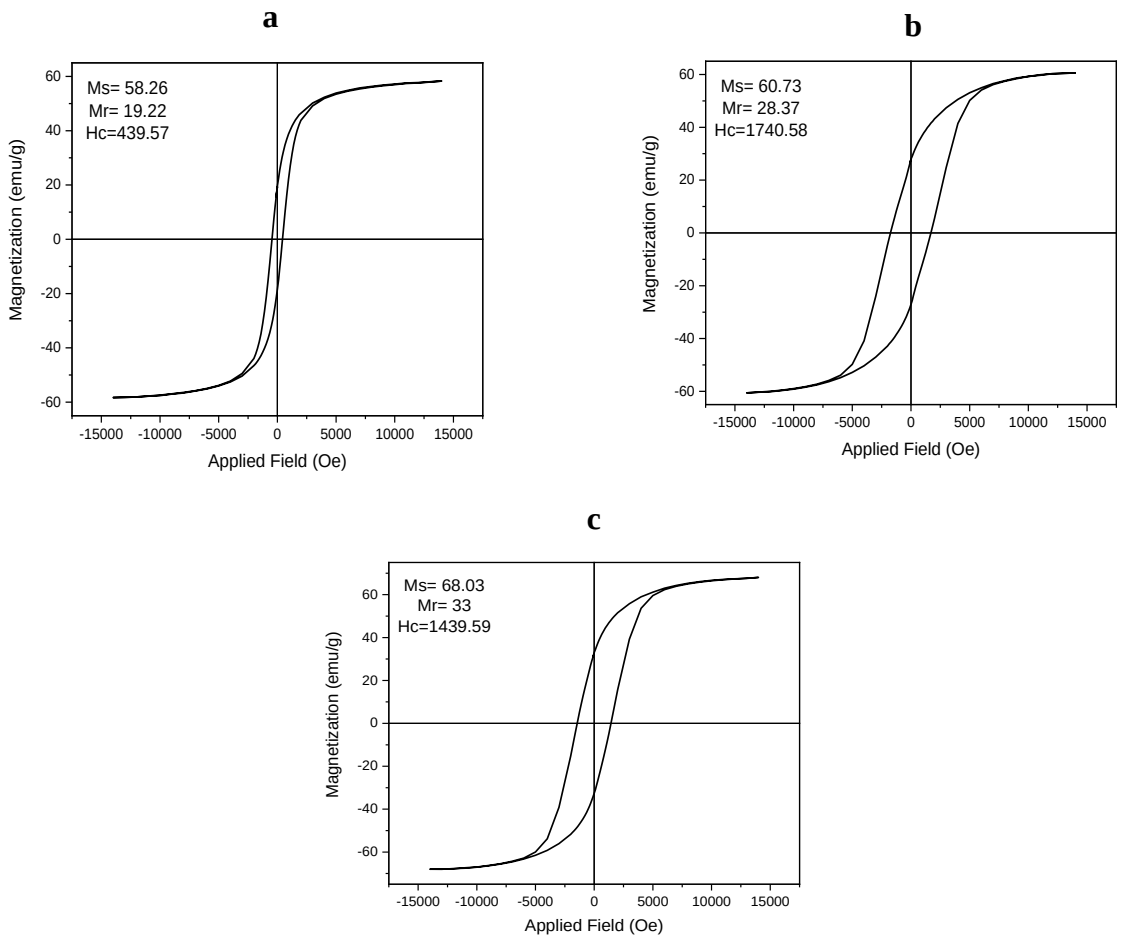

Figure 13: The hysteresis of M−H curve of $CoFe_2O_4$ with 1 M NaOH, calcined at a: 0 ºC, b:400 ºC and c:600 ºC

The method of synthesis, the cation distribution (super exchange interaction), crystal size, and shape have a significant impact on the magnetic properties of nanocrystalline spinel materials [63]. Figure (14) shows the M–H loops for the studied samples at room temperature. Magnetic characteristics of cobalt ferrite nanostructure synthesized with 3 M of NaOH calcinated at (0, 400 and 600) ^{o}C temperatures were studied under a field of 15 KOe. Saturation magnetization (M_S), remanent magnetization (M_R), and coercivity (H_C) values for cobalt ferrite nanostructure are given in Table (3). The magnetic saturation, magnetization remnant, and coercivity were all comparatively enhanced with higher calcined temperature, as seen by the M-H loops. In relation to the calcination temperature, there are two factors that influence the variation in saturation magnetization and coercivity. Higher calcination temperatures further amplify the magnetic properties' enhancement as the size of the nanoparticles increases. The phenomenon of size-dependence in magnetite nanoparticles (NPs) has been extensively studied and is well acknowledged. This phenomenon has been linked to the existence of a magnetic dead layer on the surface of the nanoparticles. Furthermore, the migration of cations to the required crystalline sites was influenced by the annealing temperature, which concurrently resulted in a decrease in the quantity of surface defect sites. The NPs samples exhibited larger coercivities when subjected to higher calcined temperatures, indicating that annealing at elevated temperatures might induce structural deformation and enhance the anisotropy of the Co ions [30].

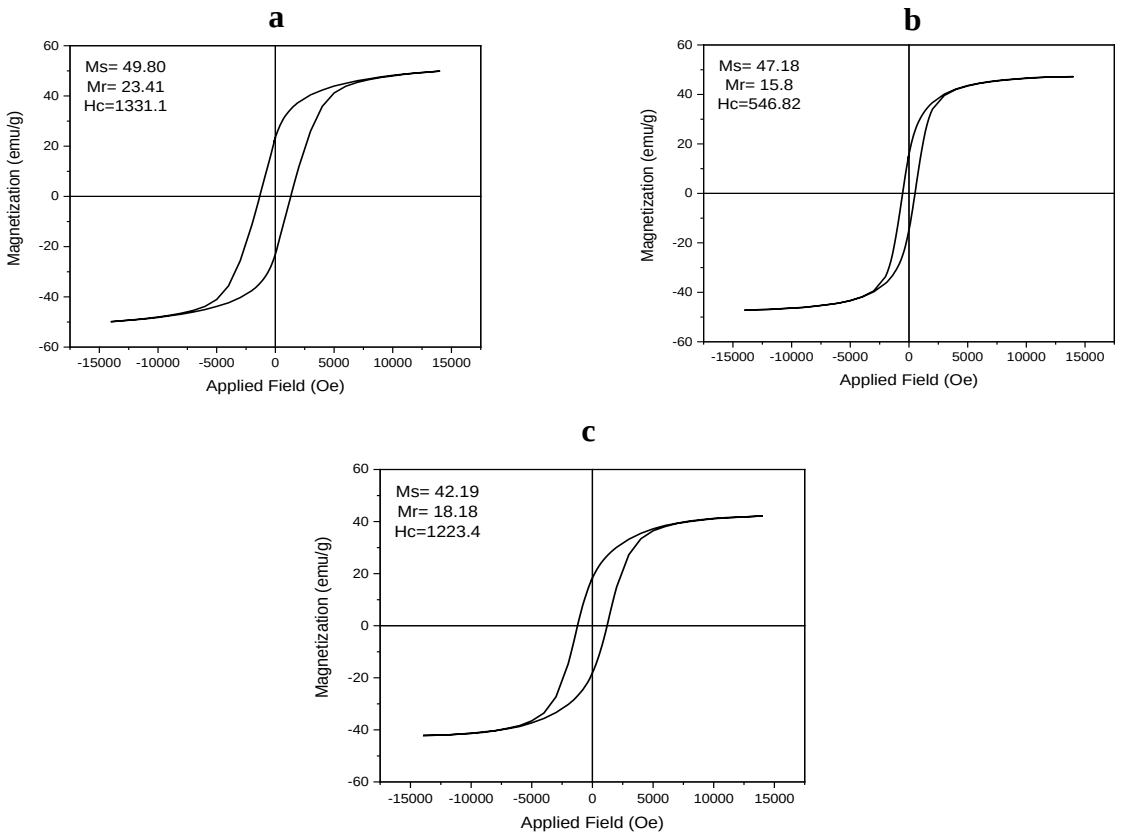

Figure 14: The hysteresis of M−H curve of $CoFe_2O_4$ with 3 M NaOH, calcined at a: 0 ^{o}C, b:400 ^{o}C and c:600 ^{o}C

Fig. (15) represents the hysteresis curves of cobalt ferrite samples synthesized with 5 M of NaOH and calcined for 0, 400 and 600 ^{o}C. The hysteresis curves show normal ferrimagnetic behaviour for all the samples. The magnetic parameters such as saturation magnetization, magneton number remnant magnetization and coercivity are obtained from the hysteresis curves. According to table (3) it was

observed that M_S is decreased with increasing calcination temperature. The loss of saturation magnetization for nanosized particles is caused by the finite-size effect of the tiny magnetic nanoparticles and the existence of a magnetic dead or antiferromagnetic layer on the surface. Additionally, unlike in bulk ferrite, the distribution of metal cations has an impact on the magnetic behavior of the ferrite-structured nanomaterials.[68]. H_C relatively decreased with increase annealing temperature because of the anisotropy barrier's anisotropy barrier's thermal fluctuations of the blocked moment and the inability to align the moments in an applied field[34]. Remanent magnetization decreased with increment of annealing temperature due the process of saturation magnetization[69]

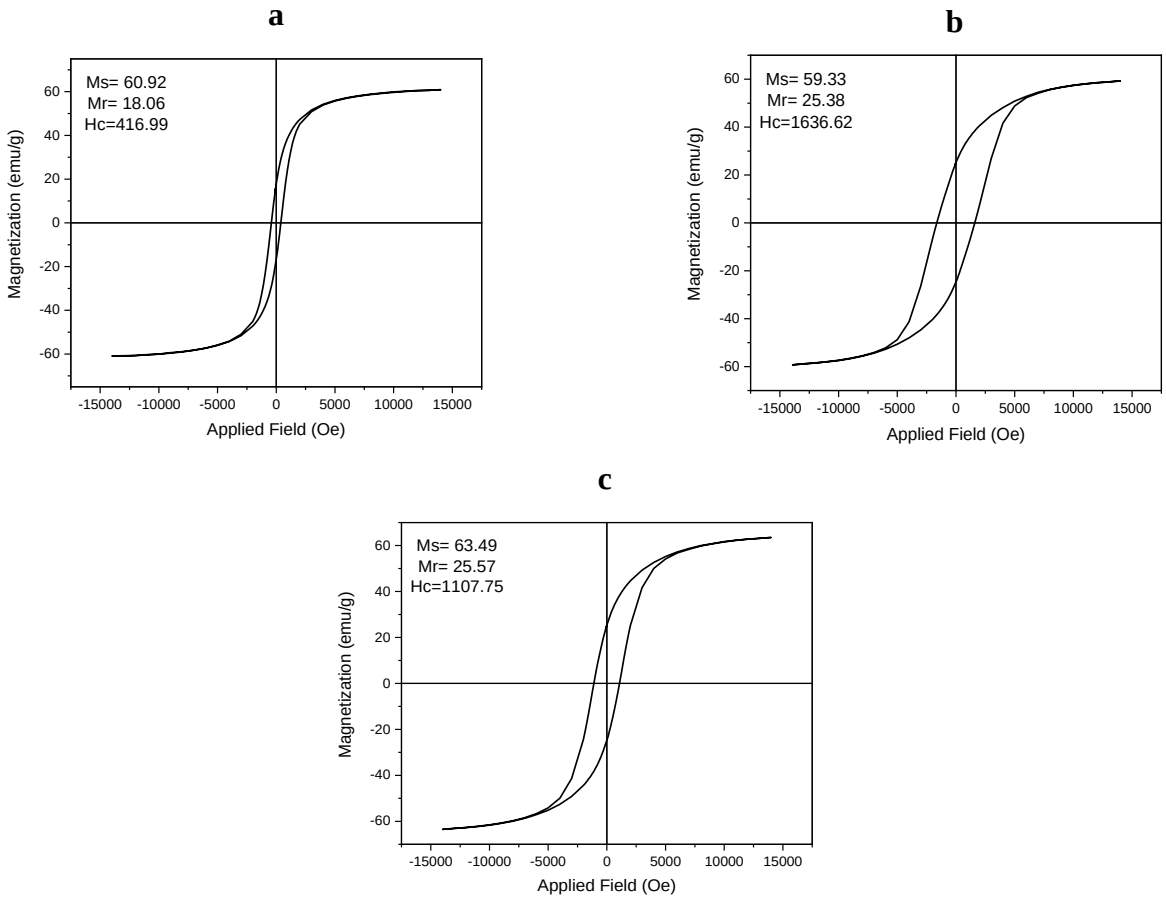

Figure 15: The hysteresis of M−H curve of $CoFe_2O_4$ with 3 M NaOH, calcined at a: 0 ºC, b:400 ºC and c:600 ºC

Table 3: Magnetic properties of the cobalt ferrite nanostructure

Sample Name		M_S (emu/g)	M_R (emu/g)	H_C (Oe)
NaOH Concentration	**Calcined Temperature ºC**			
1 M	**0**	58.26	19.22	439.57
	400	60.73	28.37	1740.58
	600	68.03	33	1439.59
3 M	**0**	60.92	18.06	416.99
	400	59.33	25.38	1636.62
	600	63.49	25.57	1107.75
5 M	**0**	49.80	23.41	1331.1
	400	47.18	15.8	546.82

	600	42.19	18.18	1223.4

3. CONCLUSION

$CoFe_2O_4$ has been prepared through hydrothermal route successfully. After obtaining $CoFe_2O_4$ powders they were calcined at 400 ^oC and 500^oC. The nanocrystalline nature regarding the synthesized particles is confirmed by XRD data, and it was discovered that the crystallite size decrease with higher annealing temperatures. Synthesized NPs had a spherical shape and size (23.6 -57.9) nm expect at 400^oC with 3M NaOH, we get nanorods shape with a diameter of 78 nm and length of 533 nm according to FESEM examination. Studies of UV-vis absorption showed a blue shift in absorption spectra. Magnetic properties of $CoFe_2O_4$ nanostructure were investigated via VSM analysis. The magnetic saturation, magnetization remnant, and coercivity were all comparatively enhanced with higher calcined temperature. The hysteresis curves show normal ferromagnetic behavior for all the samples.

References

[1] Kumar, E.R.; Jayaprakash, R.; Kumar, S. E_ect of annealing temperature on structural and magnetic properties of manganese substituted NiFe2O4 nanoparticles. Mater. Sci. Semicond. Process. **2014**, 17, 173–177.

[2] Tong, J.; Bo, L.; Li, Z.; Lei, Z.; Xia, C. Magnetic CoFe2O4 nanocrystal: A novel and e_cient heterogeneous catalyst for aerobic oxidation of cyclohexane. J. Mol. Catal. A Chem. **2009**, 307, 58–63.

[3] Rao, K.S.; Choudary, G.; Rao, K.H.; Sujatha, C. Structural and magnetic properties of ultrafine CoFe2O4 nanoparticles. Procedia Mater. Sci. **2015**, 10, 19–27.

[4] Kumar, S.; Munjal, S.; Khare, N. Metal-semiconductor transition and Seebeck inversion in CoFe2O4 nanoparticles. J. Phys. Chem. Solids **2017**, 105, 86–89

[5] Salazar-Kuri, U.; Estevez, J.O.; Silva-González, N.R.; Pal, U. Large magnetostriction in chemically fabricated CoFe2O4 nanoparticles and its temperature dependence. J. Magn. Magn. Mater. **2018**, 460, 141–145.

[6] Annie Vinosha, P.; Jerome Das, S. Investigation on the role of pH for the structural, optical and magnetic properties of cobalt ferrite nanoparticles and its e_ect on the photo-fenton activity. Mater. Today Proc. **2018**, 5, 8662–8671.

[7] Dong, N.; He, F.; Xin, J.;Wang, Q.; Lei, Z.; Su, B. Preparation of CoFe2O4 magnetic fiber nanomaterial via a template-assisted solvothermal method. Mater. Lett. **2015**, 141, 238–241.

[8] Varma, P.C.R.; Manna, R.S.; Banerjee, D.; Varma, M.R.; Suresh, K.G.; Nigam, A.K. Magnetic properties of CoFe2O4 synthesized by solid state, citrate precursor and polymerized complex methods: A comparative study. J. Alloys Compd. **2008**, 453, 298–303.

[9] Maleki, A.; Hosseini, N.; Taherizadeh, A. Synthesis and characterization of cobalt ferrite nanoparticles prepared by the glycine-nitrate process. Ceram. Int. **2018**, 44, 8576–8581.

[10] Gabal, M.A.; Al-Juaid, A.A.; El-Rashed, S.; Hussein, M.A. Synthesis and characterization of nano-sized CoFe2O4 via facile methods: A comparative study. Mater. Res. Bull. **2017**, 89, 68–78.

[11] Pourgolmohammad, B.; Masoudpanah, S.M.; Aboutalebi, M.R. Synthesis of CoFe2O4 powders with high surface area by solution combustion method: E_ect of fuel content and cobalt precursor. Ceram. Int. **2017**, 43, 3797–3803.

[12] Rajan Babu, D.; Venkatesan, K. Synthesis of nanophasic CoFe2O4 powder by self-igniting solution combustion method using mix up fuels. J. Cryst. Growth **2017**, 468, 179–184.

[13] B. Bhujun, M.T.T. Tan, A.S. Shanmugam, Results Phys. 7 (2017) 345–353.

[14] A. E. Elkholy, F. El-Taib Heakal, and Nageh K. Allam, RSC Adv. 7, 82 (2017):51888-51895.

[15] A. E. Elkholy, F. El-Taib Heakal, N. K. Allam, RSC Adv. 7 (2017) 51888-51895.

[16] M.A. Mohamed, F.M. El-badawy, H.S. El-Desoky, M.M. Ghoneim, New J. Chem. 41(2017) 11138–11147.

[17] A.S. Al-Shihri, A. Kalam, A.G. Al-Sehemi, G. Du, T. Ahmad, J. Ind. Chem. Soc 91(2014) 1861.

[18] L. Kumar and M. Kar, "Effect of La3+ substitution on the structural and magnetocrystalline anisotropy of nanocrystalline cobalt ferrite (CoFe2− xLaxO4)," *Ceram. Int.*, vol. 38, no. 6, pp. 4771–4782, 2012.

[19] N. R. A. Latiff, H. Soleimani, H. M. Zaid, N. Yahya, and M. Adil, "EFFECT OF CALCINATION ON STRUCTURAL AND MAGNETIC PROPERTIES OF CoFe2O4 SYNTHESIZED VIA CO-PRECIPITATION METHOD."

[20] F. U. Ermawati, "XRD and EDX Analyses on the Formation of MgTiO3 Phase in (Mg0. 6Zn0. 4)(Ti0. 99Sn0. 01) O3 Powders Due to Calcination Temperature Variations," in *Journal of Physics: Conference Series*, 2021, vol. 2110, no. 1, p. 12009.

[21] B. D. Cullity and S. R. Stock, "Elements of X-ray diffraction 3rd ed." Pearson Education Limited, 2014.

[22] A. Tataroglu, A. Buyukbas Ulusan, Ş. Altındal, and Y. Azizian-Kalandaragh, "A compare study on electrical properties of MS diodes with and without CoFe 2 O 4-PVP interlayer," *J. Inorg. Organomet. Polym. Mater.*, vol. 31, pp. 1668–1675, 2021.

[23] Suhad A. Hamdan, Iftikhar M. Ali "Enhancement of Hydrothermally Co_3O_4 Thin Films as H_2S Gas Sensor by Loading Yttrium Element", Baghdad Science Journal Vol.16 (1) Supplement 2019.

[24] Ikram Kamel abd Karem, Suhad A. Hamdan," The Influence off CeO_2 Concentration on some physical properties of Y_2O_3 Thin films ", Iraqi Journal of Science, Vol.(63),Issue(6) ,published on June 2022

[25] J. Hölscher, M. Saura-Múzquiz, J. Ahlburg, M. Mørch, D. K. Grønseth, and M. Christensen, "Controlling structural and magnetic properties of SrFe12O19 nanoplatelets by synthesis route and calcination time," *J. Phys. D. Appl. Phys.*, vol. 53, no. 47, p. 474002, 2020.

[26] M. Basak, M. L. Rahman, M. F. Ahmed, B. Biswas, and N. Sharmin, "Calcination effect on structural, morphological and magnetic properties of nano-sized CoFe2O4 developed by a simple co-precipitation technique," *Mater. Chem. Phys.*, vol. 264, p. 124442, 2021.

[27] N. Boda *et al.*, "Effect of rare earth elements on low temperature magnetic properties of Ni and Co-ferrite nanoparticles," *J. Magn. Magn. Mater.*, vol. 473, pp. 228–235, 2019.

[28] N. T. Lan, N. P. Duong, and T. D. Hien, "Influences of cobalt substitution and size effects on magnetic properties of coprecipitated Co–Fe ferrite nanoparticles," *J. Alloys Compd.*, vol. 509, no. 19, pp. 5919–5925, 2011.

[29] G. Márquez, V. Sagredo, R. Guillén-Guillén, G. Attolini, and F. Bolzoni, "Calcination effects on the crystal structure and magnetic properties of CoFe2O4 nanopowders synthesized by the coprecipitation method," *Rev. Mex. física*, vol. 66, no. 3, pp. 251–257, 2020.

[30] D. R. Lima *et al.*, "Employing calcination as a facile strategy to reduce the cytotoxicity in CoFe2O4 and NiFe2O4 nanoparticles," *ACS Appl. Mater. Interfaces*, vol. 9, no. 45, pp. 39830–39838, 2017.

[31] N. T. H. Lan *et al.*, "CoFe2O4 Nanomaterials: Eect of Annealing Temperature on Characterization,

Magnetic, Photocatalytic, and Photo-Fenton Properties," *Processes*, vol. 7, p. 885, 2019.

[32] I. Malinowska, Z. Ryżyńska, E. Mrotek, T. Klimczuk, and A. Zielińska-Jurek, "Synthesis of CoFe2O4 nanoparticles: the effect of ionic strength, concentration, and precursor type on morphology and magnetic properties," *J. Nanomater.*, vol. 2020, pp. 1–12, 2020.

[33] T. Sodaee, A. Ghasemi, E. Paimozd, A. Paesano, and A. Morisako, "An approach for enhancement of saturation magnetization in cobalt ferrite nanoparticles by incorporation of terbium cation," *J. Electron. Mater.*, vol. 42, pp. 2771–2783, 2013.

[34] S. Moosavi, S. Zakaria, C. H. Chia, S. Gan, N. A. Azahari, and H. Kaco, "Hydrothermal synthesis, magnetic properties and characterization of CoFe2O4 nanocrystals," *Ceram. Int.*, vol. 43, no. 10, pp. 7889–7894, 2017.

[35] L. Kumar, P. Kumar, A. Narayan, and M. Kar, "Rietveld analysis of XRD patterns of different sizes of nanocrystalline cobalt ferrite," *Int. Nano Lett.*, vol. 3, pp. 1–12, 2013.

[36] E. Mazarío, P. Herrasti, M. P. Morales, and N. Menéndez, "Synthesis and characterization of CoFe2O4 ferrite nanoparticles obtained by an electrochemical method," *Nanotechnology*, vol. 23, no. 35, p. 355708, 2012.

[37] M. Goodarz Naseri, E. B. Saion, H. Abbastabar Ahangar, A. H. Shaari, and M. Hashim, "Simple synthesis and characterization of cobalt ferrite nanoparticles by a thermal treatment method," *J. Nanomater.*, vol. 2010, 2010.

[38] R. Jayaprakash, M. S. Seehra, T. Prakash, and S. Kumar, "Effect of α-Fe2O3 phase on structural, magnetic and dielectric properties of Mn–Zn ferrite nanoparticles," *J. Phys. Chem. Solids*, vol. 74, no. 7, pp. 943–949, 2013.

[39] R. D. K. Misra, S. Gubbala, A. Kale, and W. F. Egelhoff Jr, "A comparison of the magnetic characteristics of nanocrystalline nickel, zinc, and manganese ferrites synthesized by reverse micelle technique," *Mater. Sci. Eng. B*, vol. 111, no. 2–3, pp. 164–174, 2004.

[40] N. P. Prasetya, U. Utari, Y. Iriani, and B. Purnama, "The effect of annealing temperature on the structural and magnetic properties of lanthanum doped cobalt ferrite with the bengawan solo river fine sediment as the source of Fe3+," *Key Eng. Mater.*, vol. 940, pp. 11–20, 2023.

[41] J. Feng, R. Xiong, and Y. Liu, "Effect of NaOH Concentration and Adding Sequences on Structural and Magnetic Properties of Ni 0.4 Co 0.6 Fe 2 O 4 Nanopowders Prepared Via Co-precipitation Route," *J. Supercond. Nov. Magn.*, vol. 31, pp. 2079–2088, 2018.

[42] R. Jabbar, S. H. Sabeh, and A. M. Hameed, "Synthesis and Characterization of CoFe2O4Nanoparticles Prepared by Sol-GelMethod," *Eng. Technol. J.*, vol. 38, no. 2, pp. 47–53, 2020.

[43] Z. Rahimi, H. Sarafraz, G. Alahyarizadeh, and A. S. Shirani, "Hydrothermal synthesis of magnetic CoFe 2 O 4 nanoparticles and CoFe 2 O 4/MWCNTs nanocomposites for U and Pb removal from aqueous solutions," *J. Radioanal. Nucl. Chem.*, vol. 317, pp. 431–442, 2018.

[44] N. M. Refat, M. Y. Nassar, and S. A. Sadeek, "A controllable one-pot hydrothermal synthesis of spherical cobalt ferrite nanoparticles: synthesis, characterization, and optical properties," *RSC Adv.*, vol. 12, no. 38, pp. 25081–25095, 2022.

[45] S. Pauline and A. P. Amaliya, "Synthesis and characterization of highly monodispersive CoFe2O4 magnetic nanoparticles by hydrothermal chemical route," *Arch. Appl. Sci. Res.*, vol. 3, no. 5, pp. 213–223, 2011.

[46] A. K. Agustina, J. Utomo, E. Suharyadi, T. Kato, and S. Iwata, "Effect of synthesis parameters on

crystals structures and magnetic properties of cobalt nickel ferrite nanoparticles," in *IOP Conference Series: Materials Science and Engineering*, 2018, vol. 367, no. 1, p. 12006.

[47] R. R. Febriani, N. P. Prasetya, N. A. Wibowo, A. Supriyanto, A. H. Ramelan, and B. Purnama, "Sodium-hydroxide molarities influence the structural and magnetic properties of strontium-substituted cobalt ferrite nanoparticles produced via co-precipitation," *Kuwait J. Sci.*, 2023.

[48] D. E. Saputro, S. Budiawanti, S. W. Sukarsa, D. T. Rahardjo, and B. Purnama, "THE EFFECT OF MODIFY NaOH CONCENTRATION ON THE STRUCTURE AND MAGNETIC PROPERTIES IN CO-PRECIPITATED NANOCRYSTALLINE BISMUTH SUBSTITUTED COBALT FERRITE," *J. Teknol.*, vol. 84, no. 3, pp. 9–15, 2022.

[49] S. Agrawal, A. Parveen, and A. Azam, "Structural, electrical, and optomagnetic tweaking of Zn doped CoFe2− xZnxO4− δ nanoparticles," *J. Magn. Magn. Mater.*, vol. 414, pp. 144–152, 2016.

[50] F. Li, T. Kong, W. Bi, D. Li, Z. Li, and X. Huang, "Synthesis and optical properties of CuS nanoplate-based architectures by a solvothermal method," *Appl. Surf. Sci.*, vol. 255, no. 12, pp. 6285–6289, 2009.

[51] A. Singh, H. Gangwar, and B. S. Dehiya, "Synthesis and microstructural characterization of pure cobalt ferrite for DC electrical study," *J Mater Sci Mech Eng*, vol. 4, pp. 136–141, 2017.

[52] [52] S. Saleem *et al.*, "Investigating the impact of Cu2+ doping on the morphological, structural, optical, and electrical properties of CoFe2O4 nanoparticles for use in electrical devices," *Materials (Basel).*, vol. 15, no. 10, p. 3502, 2022.

[53] P. Dhiman *et al.*, "Constructing a Visible-Active CoFe2O4@ Bi2O3/NiO Nanoheterojunction as Magnetically Recoverable Photocatalyst with Boosted Ofloxacin Degradation Efficiency," *Molecules*, vol. 27, no. 23, p. 8234, 2022.

[54] L. Velayutham *et al.*, "Photocatalytic and antibacterial activity of CoFe2O4 nanoparticles from hibiscus rosa-sinensis plant extract," *Nanomaterials*, vol. 12, no. 20, p. 3668, 2022.

[55] D. Yuliantika, A. Taufiq, A. Hidayat, Sunaryono, N. Hidayat, and S. Soontaranon, "Exploring structural properties of cobalt ferrite nanoparticles from natural sand," in *IOP Conference Series: Materials Science and Engineering*, 2019, vol. 515, p. 12047.

[56] H. A Kareem *et al.*, "Synthesis and Characterization of CoFe2O4 Nanoparticles and Its Application in Removal of Reactive Violet 5 from Water," *J. Nanostructures*, vol. 12, no. 3, pp. 521–528, 2022.

[57] N. M. Al-Hada, H. M. Kamari, A. A. Baqer, A. H. Shaari, and E. Saion, "Thermal calcination-based production of SnO2 nanopowder: an analysis of SnO2 nanoparticle characteristics and antibacterial activities," *Nanomaterials*, vol. 8, no. 4, p. 250, 2018.

[58] M. H. Habibi and H. J. Parhizkar, "FTIR and UV–vis diffuse reflectance spectroscopy studies of the wet chemical (WC) route synthesized nano-structure CoFe2O4 from CoCl2 and FeCl3," *Spectrochim. Acta Part A Mol. Biomol. Spectrosc.*, vol. 127, pp. 102–106, 2014.

[59] I. Sugihartono *et al.*, "The influence of calcination temperature on optical properties of ZnO nanoparticles," in *AIP Conference Proceedings*, 2019, vol. 2169, no. 1.

[60] S. Iqbal *et al.*, "Development of TiO2 decorated Fe2O3QDs/g-C3N4 Ternary Z-scheme photocatalyst involving the investigation of phase analysis via strain mapping and its photocatalytic performance under visible light illumination," *Res. Chem. Intermed.*, pp. 1–36, 2023.

[61] H. Hamad, M. Abd El-Latif, A. E.-H. Kashyout, W. Sadik, and M. Feteha, "Synthesis and characterization of core–shell–shell magnetic (CoFe 2 O 4–SiO 2–TiO 2) nanocomposites and TiO 2 nanoparticles for the evaluation of photocatalytic activity under UV and visible irradiation," *New J.*

Chem., vol. 39, no. 4, pp. 3116–3128, 2015.

[62] J. Thomas *et al.*, "Synthesis of cobalt ferrite nanoparticles by constant pH co-precipitation and their high catalytic activity in CO oxidation," *New J. Chem.*, vol. 41, no. 15, pp. 7356–7363, 2017.

[63] E. Pervaiz, I. H. Gul, and H. Anwar, "Hydrothermal synthesis and characterization of CoFe 2 O 4 nanoparticles and nanorods," *J. Supercond. Nov. Magn.*, vol. 26, pp. 415–424, 2013.

[64] M. ÖZDİNÇER, S. DURMUŞ, and A. DALMAZ, "Magnetic spinel-type CoFe2O4 nanoparticles: synthesis and investigation of structural, morphological properties," *Süleyman Demirel Üniversitesi Fen Bilim. Enstitüsü Derg.*, vol. 21, no. 2, pp. 311–315, 2017.

[65] Q. Liu, J. Sun, H. Long, X. Sun, X. Zhong, and Z. Xu, "Hydrothermal synthesis of CoFe2O4 nanoplatelets and nanoparticles," *Mater. Chem. Phys.*, vol. 108, no. 2–3, pp. 269–273, 2008.

[66] [66] H. T. K. N. Duong Hong Quyen, Dam Ngoc Anh, "Effect of Reaction pH on Characterization of Co-precipitated Cobalt ferrite Nanoparticles," *Int. J. Sci. Res. Sci. Eng. Technol.*, vol. 4, no. 8, 2018.

[67] Т. Р. Татарчук, "Structural, Optical, and Magnetic Properties of Zn-Doped CoFe2O4 Nanoparticles," 2017.

[68] F. Zhang, R. L. Su, L. Z. Shi, Y. Liu, Y. N. Chen, and Z. J. Wang, "Hydrothermal Synthesis of CoFe2O4 nanoparticles and their magnetic properties," in *Advanced Materials Research*, 2013, vol. 821, pp. 1358–1361.

[69] D. E. Saputro, U. Utari, and B. Purnama, "Effect of bismuth substitution on magnetic properties of CoFe2O4 nanoparticles: Study of synthesize using coprecipitation method," *J. Phys. Theor. Appl*, vol. 3, no. 9, 2019.